Optimized thermal imaging with a singlet and pupil plane encoding: experimental realization

Gonzalo Muyo[1], Amritpal Singh[2], Mathias Andersson[2], David Huckridge[3] and Andy Harvey[1]
[1]School of Engineering and Physical Sciences, Heriot-Watt University, Edinburgh, EH14 4AS, Scotland, United Kingdom
[2]Development and Technology Sensors, SAAB Bofors Dynamics AB, SE-402 51 Göteborg, Sweden.
[3]QinetiQ, Malvern, WR14 3PS, United Kingdom.

ABSTRACT

Pupil plane encoding has shown to be a useful technique to extend the depth of field of optical systems. Recently, further studies have demonstrated its potential in reducing the impact of other common focus-related aberrations (such as thermally induced defocus, field curvature, etc) which enables to employ simple and low-cost optical systems while maintaining good optical performance. In this paper, we present for the first time an experimental application where pupil plane encoding alleviates aberrations across the field of view of an uncooled LWIR optical system formed by F/1, 75mm focal length germanium singlet and a 320x240 detector array with 38-micron pixel. The singlet was corrected from coma and spherical aberration but exhibited large amounts of astigmatism and field curvature even for small fields of view. A manufactured asymmetrical germanium phase mask was placed at the front of the singlet, which in combination with digital image processing enabled to increase significantly the performance across the entire field of view. This improvement is subject to the exceptionally challenging manufacturing of the asymmetrical phase mask and noise amplification in the digitally restored image. Future research will consider manufacturing of the phase mask in the front surface of the singlet and a real-time implementation of the image processing algorithms.

Keywords: Pupil plane encoding, thermal imaging, singlet, noise amplification.

1. INTRODUCTION

In recent years, the introduction of a especial phase mask in the aperture stop of an incoherent optical system has shown to increase in a significant way the tolerance to manufacturing inaccuracies and various aberrations, in particular defocus related aberrations such as temperature-induced defocus, field curvature, chromatic aberration, astigmatism, etc [1-5]. The fundamental concept of this technique involves a phase mask that introduces a controlled distortion in the transmitted wavefront so as to produce a distinctively blurred image with a specific point spread function (PSF). The intensity distribution of the PSF, which normally is not rotationally symmetric, is practically constant to aberrations and across a region near the image focal plane. Post-detection digital signal processing is required in order to decode or remove the blur from the detected image. In general, the blur of antisymmetric phase masks gives rise to a modulation-transfer-function (MTF) which exhibits no zeros throughout the designed-tolerance range. The absence of nulls prevents loss of spatial frequencies and a high fidelity image can be obtained using an inversion filter in the digital processing.

The extended performance of an optical/digital imaging system with pupil plane encoding is subject to some limitations, namely, substantial noise amplification in the digitally recovered image and difficulty in manufacturing to a significant level of precision an antisymmetric phase mask with a peak-to-valley height of just a few microns. Nevertheless, it is the reduction in the signal-to-noise ratio of the restored image that sets a practical limit to the magnitude of aberration tolerance.

In our previous work [6], we considered the possibility of using a pupil phase mask to reduce the lens count of a conventional two-element infrared imaging system whilst maintain a high imaging performance. The lens count was

reduced to a single element (the front meniscus lens), in which the on-axis performance was diffraction-limited but rapidly reduced by strong astigmatism and field curvature at small fields of view. We showed by means of modelling that by introducing an antisymmetric germanium phase mask in the front surface of the singlet together with digital image processing, allowed increasing imaging performance across the field of view.

In this paper, we present an experimental realization of a hybrid infrared imaging system based on the theoretical model shown in the past [6]. The new optical/digital imaging system combines a singlet with a phase mask, both made with germanium, and a long-wave uncooled infrared detector. At this stage, the phase mask is designed as a separated element in the system but future work aims to include the phase mask on the first surface of the singlet. In that way, the system will further benefit from low weight, low cost and small optics. In addition, at this phase of the project the restoration of the detected images is not carried out in real-time.

The outline of the paper is as follows: in section two, we give a brief review of the characteristics of the ZEMAX-modelled singlet imaging system and the challenges involved in the manufacture of the germanium phase mask using single-point diamond machining. Also, a comparison between the shape and depth of the designed and manufactured phase masks is provided. In section three, a description of the digital post-detection processing employed to deconvolve the real encoded infrared images is presented along with a qualitative evaluation of the restored images. Finally, conclusions and future work are presented.

2. EXPERIMENTAL PUPIL PLANE ENCODING SINGLET

2.1. Review of the model

It was demonstrated in Ref. [6] that a phase mask with the appropriate shape and phase distortion, together with digital image processing, allowed the reduction of aberrations and improved imaging performance across the field of view in the proposed singlet. The singlet is displayed in Figure 1(a). The MTFs of the singlet for various fields of view up to 7.5 degrees are shown in Figure 1(b), note how the diffraction-limited on-axis performance rapidly drops at small fields of view. The phase mask was based on a derivation by Prasad *et. al* [2] and its antisymmetric shape is given by

$$\theta(x, y) = \alpha\left(x^3 + y^3\right) + \beta\left(x^2 y + x y^2\right) \tag{1}$$

where |x|<1, |y|<1 are normalised co-ordinates and α and β are real variables that control the distortion or optical path difference introduced in the wavefront.

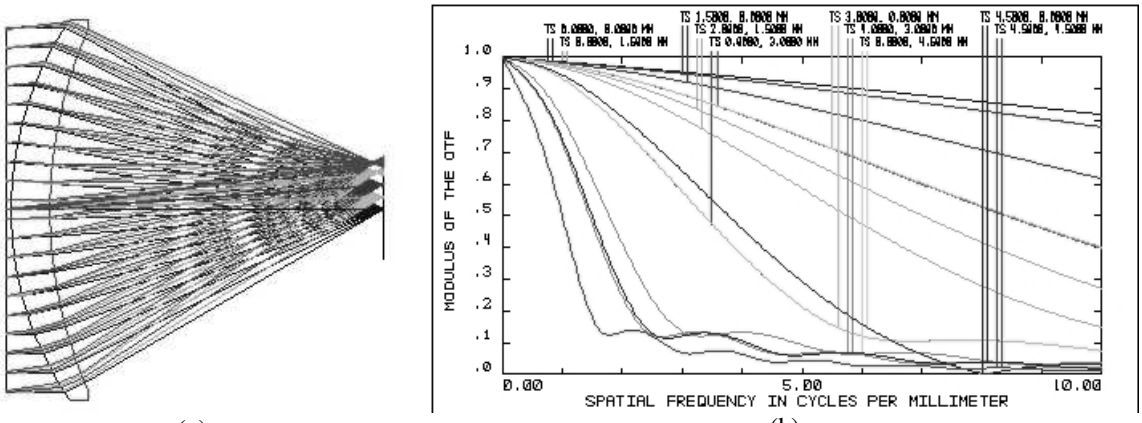

(a) (b)

Figure 1. (a) Singlet layout made of germanium, effective focal length f=75 mm, F/1. (b) Singlet's MTF performance for various fields of view (0 to 7.5 degrees).

The phase mask parameters α and β were optimized to correct up to 6 waves (λ=10.5 microns) of aberration which corresponded to the wavefront aberration of a field of view of approximately 7.5 degrees. Within the area where the

aberrations were corrected, the PSFs of the singlet/phase mask system remained practically invariant and the MTFs contained no nulls (within the detector passband). The MTFs of the pupil plane encoding imaging system are illustrated in Figure 2(a). The suppression in the MTFs is determined by the controlled wavefront distortion introduced by α and β. It can be observed from the MTF plots that by applying a simple inverse digital filter we can recover an almost diffraction-limited optical system. However, this extended performance is significantly limited by noise amplification in the digitally restore images. As we will see in the next section, restoration algorithms must be chosen accordingly in order to prevent noise amplification to unacceptable levels.

2.2. Manufacture of the singlet and phase mask

An F/1 germanium singlet, effective focal length of 75mm, which included an even asphere in the second surface of the element was manufactured, see Figure 1(a). The singlet was corrected for coma and spherical aberration but limited by astigmatism and field curvature.

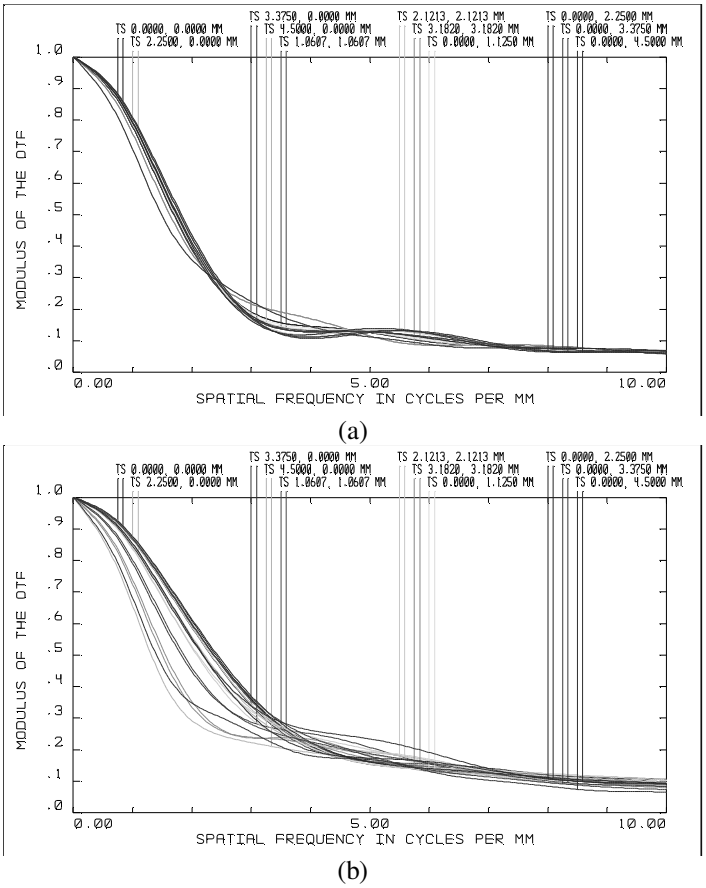

Figure 2. MTF performance for various fields of view ranging from 0 to 7.5 degrees for (a) singlet with the designed phase mask (b) with Zernike polynomial fitting based on the manufactured phase mask. The difference is negligible.

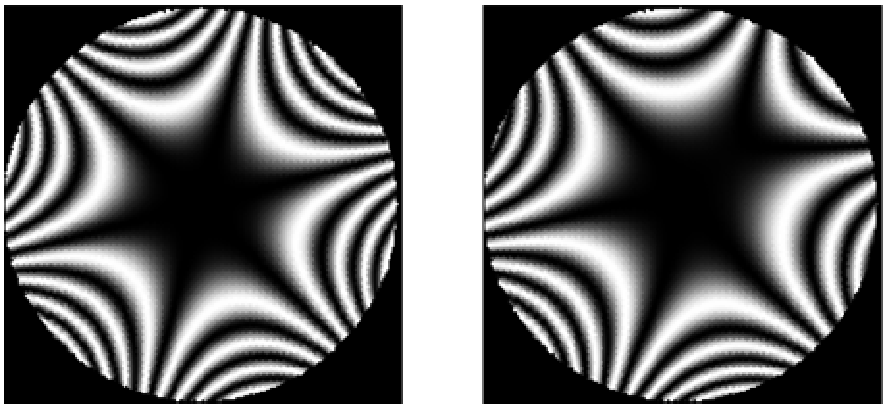

(a) (b)

Figure 3. (a) Wavefront interferograms produced by the designed phase mask given by Eq.(1) and (b) by the Zernike polynomial fitting of the manufactured phase mask.

Despite the difficulties and challenges involved in the manufacturing process, the produced phase mask presented very little deviation from the originally designed phase mask. The physical peak-to-valley distance of the manufactured phase mask was 24 microns, which was slightly inferior to that of the designed mask. This small reduction in the phase height resulted in a small loss of aberration tolerance, thus fields of view near the edge at 7.5 degrees became in some way affected by the weaker manufactured phase mask. Figure 3 shows a comparison of the interferograms generated by the designed and manufactured phase masks. It can be observed that a minor deformation from the ideal shape was introduced during the manufacturing process.

In addition to manufacturing a phase mask with a peak-to-valley height of 24 microns, another phase mask with identical shape but with less surface peak-to-valley sag (~16 microns) was manufactured. This mask corresponds to approximately 3 waves of aberration correction.

3. RESTORATION ALGORITHMS AND RESULTS

The PSF of the optical system is, as mentioned above, shift-variant. Especially towards the edges of the field of view (FOV), the PSF changes rapidly. Due to the spatial variation of the optical PSF, it is not possible to use deconvolution schemes for restoration of the whole encoded image. In the central part of the FOV, where the optimised phase mask has reduced the astigmatism of the singlet and hence the PSF is more or less constant, deconvolution can actually be expected to yield an acceptable restoration. However, to deal with the blur also outside the optimised circular area [9], one needs to solve the Fredholm integral equation, in which we take into account the spatial variation of the PSF,

$$i(s) = \int h(s,t)o(t)dt + n\,.$$

The detected image i is formed by the original image o and the blurring function h, s and t are 2-D spatial coordinates and n is an additive noise term. We have used the Van Cittert algorithm [7] to approximate the original image o

$$x^n = x^{n-1} + \beta(b - Hx^{n-1})\,,$$

where x is the estimate of the original image, b is the blurred image and H is the PSF matrix. The images, originally of size $m \times n$, are reshaped into column-vectors of size $mn \times 1$. H is a matrix of size $mn \times mn$ where each row corresponds to the PSF in one point in the image plane. The calculation is iterated until an image with sufficient quality is produced.

The PSFs, used in the restoration process, were calculated by modelling the manufactured singlet and phase mask in ZEMAX. By modelling the manufactured optical elements in ZEMAX, we were able to increase the accuracy and reliability of the restoration process. In order to model the manufactured phase mask in ZEMAX a Zernike polynomial fitting was applied into the germanium phase mask. The Zernike coefficient obtained in the fitting generated a simulated phase mask whose RMS with respect to the real manufactured phase mask resulted to be less than 2%. This minute error was assumed to be negligible as it can be observed in Figure 2(b). The MTFs for the Zernike-fitted phase mask are practically identical to those of the originally designed phase mask, which are displayed in Figure 2(a). For practical reasons, it was not possible to provide the restoration algorithm with PSFs at each image pixel. Instead the PSFs were calculated at certain field intervals. The filter response of the PSF at points situated between field intervals was approximated through a linear interpolation between the four nearest known PSF samples.

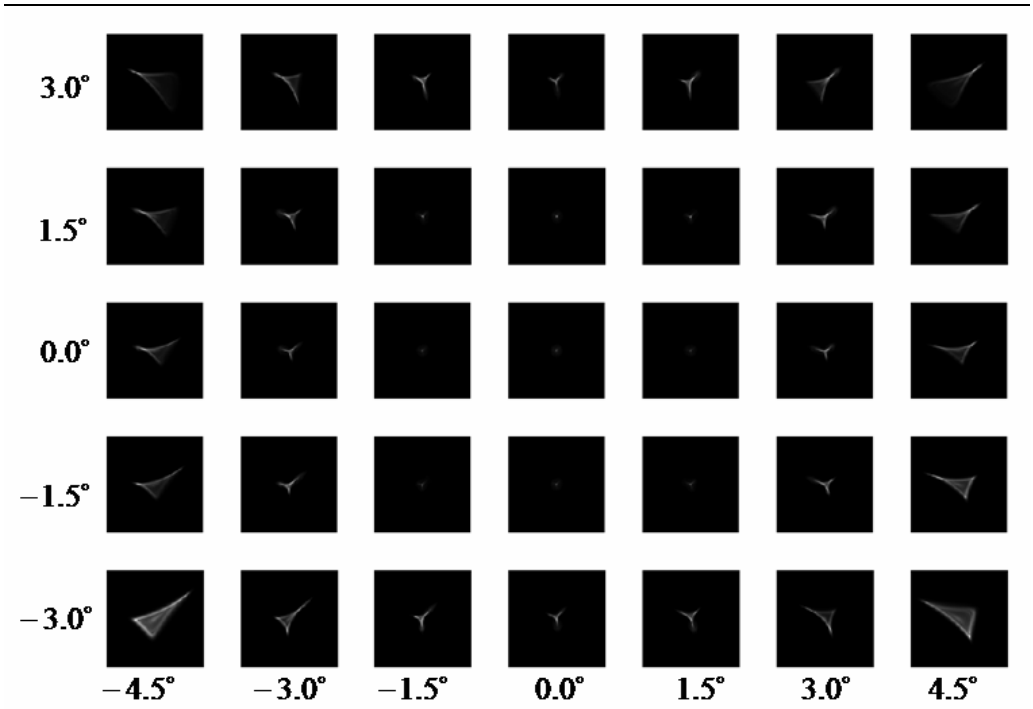

Figure 4. The spatial variation of the PSF is shown for a ~3λ phase mask. Each PSF box corresponds to a 1.95-by-1.95 mm square in the image plane. The distance between the PSF boxes is not to scale. The total FOV of the system is 9.2° by 7°.

In the experimental setup an uncooled IR detector array with 320x240 pixels and a pixel size of 38 microns was placed at the Gaussian image plane. The total FOV of the system is 9.2 by 7 degrees. The operating wavelengths were 9-12 μm. There was a light snow fall during the imaging session, resulting in rather small contrasts. The non uniformity correction (NUC) was not able to completely remove the fix pattern noise (FPN). Figure 5 to Figure 7 shows a few examples of the resulting images. Stationary scenes of a building, Figure 5 and Figure 6, were imaged both with and without the phase mask. In these figures we also show the results of the restoration using the above Van Cittert algorithm, which takes into account the spatial variation of the PSF. As a reference, we also show the results of restoration with the Lucy-Richardson deconvolution (LRD), which only uses the central PSF.

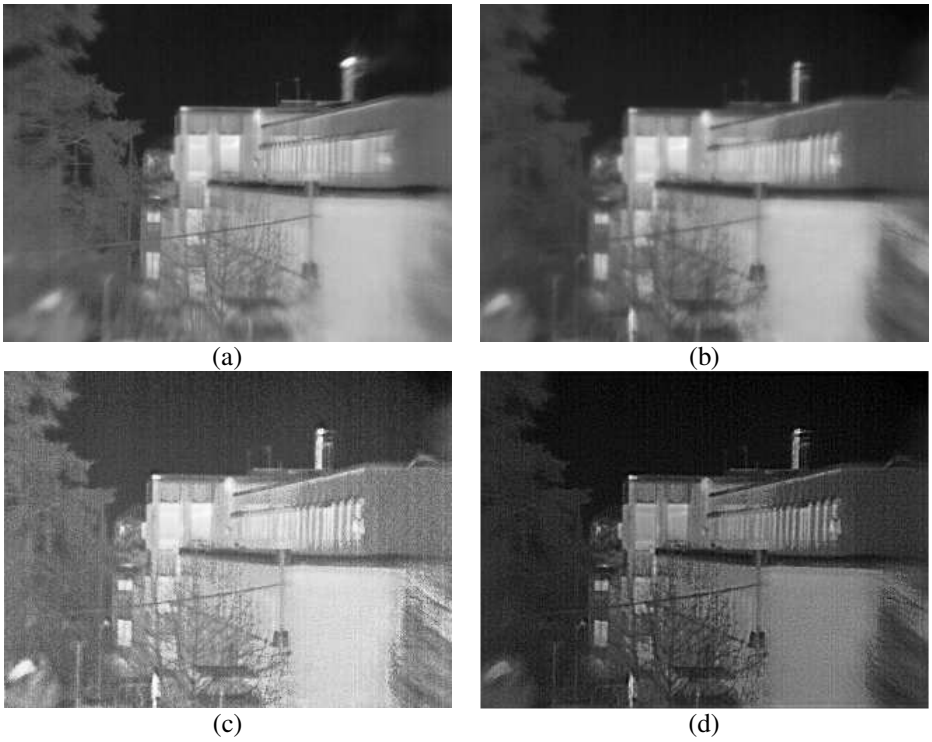

(a) (b)

(c) (d)

Figure 5. (a) Image taken with only the singlet at the best on-axis focus. (b) Image taken with the singlet and a ~3λ phase mask, the same focusing position as in (a). (c) The resulting image after shift-variant restoration. (d) The resulting image after Lucy-Richardson deconvolution, utilizing only the central PSF.

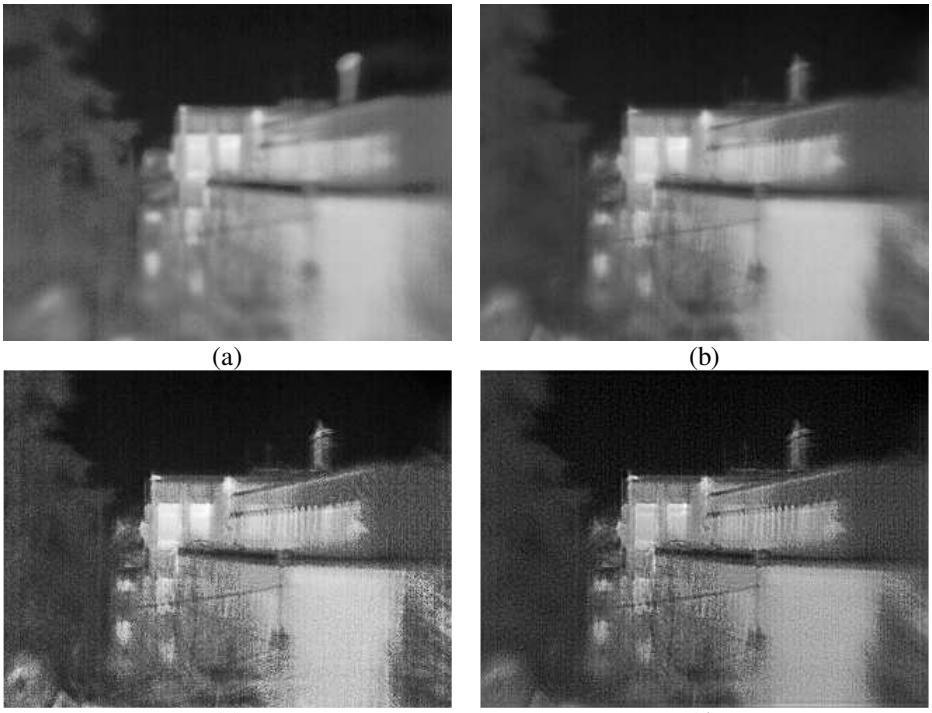

(a) (b)

(c) (d)

Figure 6. Same scene as in Figure 4 but with defocused optics. (a) singlet only. (b) singlet and ~3λ phase mask. (c) Restored using the space-variant PSF. (d) Restored using LRD and the central PSF.

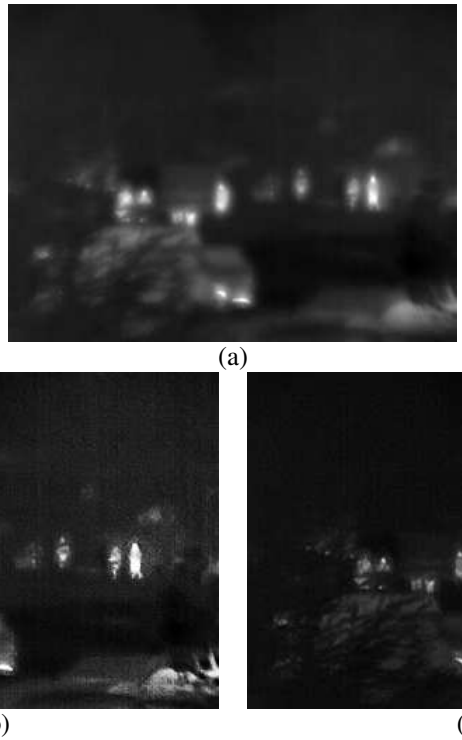

(a)

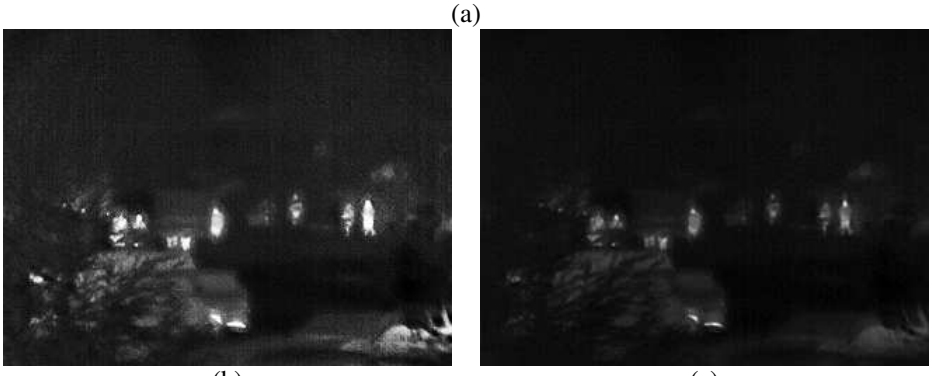

(b) (c)

Figure 7. Image taken with the singlet and the ~6λ phase mask. (b) Restored image using the shift-variant PSF. (c) Restored by LRD, utilizing the central PSF only.

From Figure 5 and Figure 6 we see that the inclusion of the phase mask leads to more blurry images. The PSF stabilization properties of the phase mask is most clearly seen in the defocused case in Figure 6. Comparing Figure 5 and Figure 6, the defocusing of the optics leads to a more blurry image in Figure 6a (singlet only). As the phase mask is included, Figure 5b and Figure 6b, defocusing only leads to very small changes in the resulting image.

The restoration, both Van Cittert and LRD, clearly enhance the image details. Unfortunately the restoration process also amplifies noise and thereby lowers the signal-to-noise-ratio (SNR). We should note here that the uncooled detector in combination with the weather conditions leads to excessive amounts of fix pattern noise, which is exaggerated in the restoration process. A better non-uniformity correction and/or higher contrast input images can be expected to yield even better restored images, with respect to image detail and SNR. To some extent, the noise can be reduced in the restored images by adaptive image processing, such as a Wiener filtering or wavelets based noise reduction algorithms [9].

Lucy-Richardson deconvolution works surprisingly well in the central part of the FOV and exhibit moderate noise amplification. Towards the edges of the field of view LRD is not able to deblur the images; this is especially obvious in the defocused case in Figure 6. The Van Cittert algorithm, taking into account the varying PSF, does a better job towards the edges of the FOV but results in somewhat higher noise amplification.

The lower noise amplification in the LRD restoration is partly due to the fact that it only deals with a rather nice, i.e. small, PSF and partly because the implementation uses regularization, between iterations, to suppress noise. At the time being, the Van Cittert implementation has no regularizing mechanisms and also deals with rather large PSFs at the edges of the FOV.

4. CONCLUSIONS

We have described what we believe is the first experimental realization of the potential of using pupil plane encoding together with digital signal processing to reduce the number of optical elements and mitigate aberrations in an IR imaging system. A singlet and phase masks with various peak-to-valley heights were manufactured in Germanium by means of single point diamond machining. Despite the difficulties in manufacturing an antisymmetric shape with just a few microns of surface sag, the phase mask was produced closely in agreement to the original design characteristics. We have shown that the combination of pupil plane encoding and digital restoration clearly enhances image sharpness across the full field of a single-lens thermal imaging system and that this can be achieved with an acceptable reduction in the signal-to-noise ratio. In the regions of the image where the PSF was practically invariant with field of view, the Lucy-Richardson deconvolution technique restored the images rather well with moderate noise amplification. Outside this region, towards the edges of the field of view, the technique failed to remove the spatially varying blur. In contrast, the Van Cittert algorithm, which considers the varying PSF, performed significantly better towards the edges but resulted in higher noise amplification. However, we judge that the image quality after restoration is still superior in all of the considered cases to that produced without pupil plane encoding.

To avoid the effect of thermal defocus, as is evident with this Germanium singlet, future work aims to manufacture in a pupil-plane-encoding singlet from chalcogenide, with the encoding phase function incorporated into the front surface. In this case, the manufacturing of the singlet will benefit from low-cost moulding techniques.

ACKNOWLEDGEMENTS

This work was supported by the Ministry of Defence (UK), Swedish Defence Material Administration (FMV), QinetiQ (Malvern, UK), Qioptiq (St. Asaph, UK) and Saab Bofors Dynamics AB (Sweden).

We are especially indebted to our project partners Qioptiq for the manufacturing and testing of the phase mask and singlet.

We are also very grateful to FLIR systems for providing the IR detector as well as lab facilities.

REFERENCES

1. E. Dowski and T. W. Cathey, "Extended depth of field through wavefront coding," Appl. Opt. **34**, 1859-1866 (1995).

2. S. Prasad, T. Torgersen, V. P. Pauca, R. Plemmons, J. van der Gracht, "Engineering the Pupil Phase to Improve Image Quality," in Proceedings of the SPIE, Vol. 5108 *Visual Information Processing XII*, edited by Z. Rahman, R. Schowengrdt, and S. Reichenbach (SPIE, Wellingham, WA, 2003), pp. 1-12.

3. K. Kubala, E. R. Dowski, and W. T. Cathey, "Reducing complexity in computational imaging systems," Opt. Express **11**, 2102-2108 (2003).

4. S. Mezouari, G. Muyo and A. R. Harvey, "Amplitude and phase filters for mitigation of defocus and third-order aberrations," Proc SPIE 4768, 21-31 (2003).

5. G. Muyo, A. R. Harvey, "Wavefront coding for athermalization of infrared imaging systems," Proc. SPIE Vol. 5612, p. 227-235 (2004).

6. G. Muyo, A. R. Harvey, A. Singh, "High-performance thermal imaging with a singlet and pupil plane encoding," Proc. SPIE Vol. 5987, 59870I, (2005).

7. P. A. Janson (editor), *Deconvolution of Images and Spectra*, Academic Press, 2nd edition, 1997

8. R.C. Gonzales and R.E. Woods, Digital Image Processing. 2nd Ed., Prentice Hall, 2002.